

Communication

Mo₂C as Pre-Catalyst for the C-H Allylic Oxygenation of Alkenes and Terpenoids in the Presence of H₂O₂

Michael G. Kallitsakis¹, Dimitra K. Gioftsidou¹, Marina A. Tzani¹ , Panagiotis A. Angaridis¹,
Michael A. Terzidis^{2,*}  and Ioannis N. Lykakis^{1,*} 

¹ Department of Chemistry, Aristotle University of Thessaloniki, University Campus, 54124 Thessaloniki, Greece; kallitsos29@gmail.com (M.G.K.); dimgpan10@yahoo.gr (D.K.G.); marina_tzani@hotmail.com (M.A.T.); panosangaridis@chem.auth.gr (P.A.A.)

² Department of Nutritional Sciences and Dietetics, International Hellenic University, Sindos Campus, 57400 Thessaloniki, Greece

* Correspondence: mterzidis@ihu.gr (M.A.T.); lykakis@chem.auth.gr (I.N.L.)

Abstract: In this study, commercially available molybdenum carbide (Mo₂C) was used, in the presence of H₂O₂, as an efficient pre-catalyst for the selective C-H allylic oxygenation of several unsaturated molecules into the corresponding allylic alcohols. Under these basic conditions, an air-stable, molybdenum-based polyoxometalate cluster (Mo-POM) was formed in situ, leading to the generation of singlet oxygen (¹O₂), which is responsible for the oxygenation reactions. X-ray diffraction, SEM/EDX and HRMS analyses support the formation mainly of the Mo₆O₁₉²⁻ cluster. Following the proposed procedure, a series of cycloalkenes, styrenes, terpenoids and methyl oleate were successfully transformed into hydroperoxides. After subsequent reduction, the corresponding allylic alcohols were produced with good yields and in lab-scale quantities. A mechanistic study excluded a hydrogen atom transfer pathway and supported the *twix*-selective oxygenation of cycloalkenes on the more sterically hindered side via the ¹O₂ generation.

Keywords: molybdenum carbide; polyoxometalates; singlet oxygen; C-H allylic activation; alkenes oxygenation; terpenoids; lipids



Citation: Kallitsakis, M.G.; Gioftsidou, D.K.; Tzani, M.A.; Angaridis, P.A.; Terzidis, M.A.; Lykakis, I.N. Mo₂C as Pre-Catalyst for the C-H Allylic Oxygenation of Alkenes and Terpenoids in the Presence of H₂O₂. *Organics* **2022**, *3*, 173–186. <https://doi.org/10.3390/org3030014>

Academic Editor: Pierluca Galloni

Received: 11 May 2022

Accepted: 24 June 2022

Published: 4 July 2022

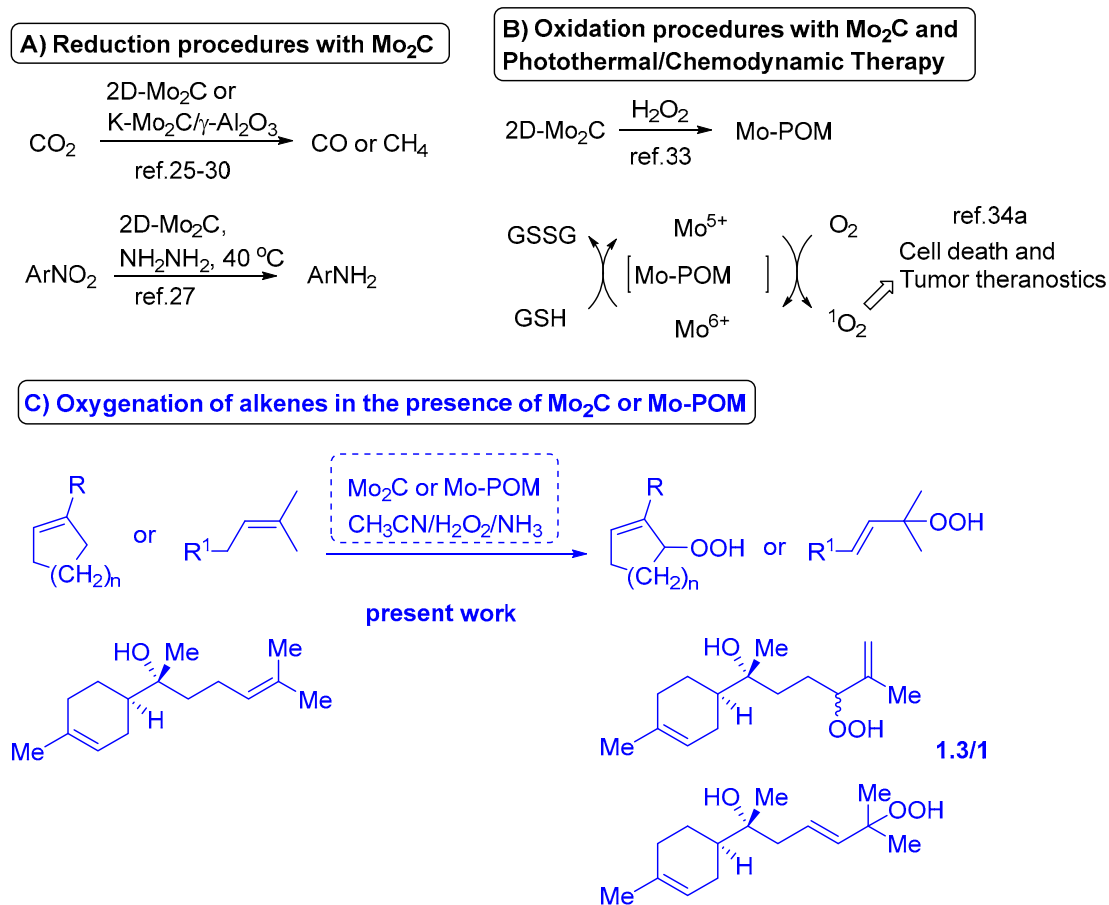
Publisher's Note: MDPI stays neutral with regard to jurisdictional claims in published maps and institutional affiliations.



Copyright: © 2022 by the authors. Licensee MDPI, Basel, Switzerland. This article is an open access article distributed under the terms and conditions of the Creative Commons Attribution (CC BY) license (<https://creativecommons.org/licenses/by/4.0/>).

1. Introduction

In recent years, the use of low cost, renewable and bio-based materials as catalysts has received increasing attention in the field of green and sustainable chemistry. Among the widely used, early-transition-metal catalytic materials, the carbides of the earth-abundant Mo and W (Mo₂C and W₂C) [1–3] feature catalytic properties similar to those of noble metals [4,5]. Several catalytic processes, including Fischer–Tropsch (FT) synthesis [6,7], methane dry reforming [8], water-gas shift (WGS) reaction [9,10], alkenes [11] and CO/CO₂ hydrogenation into value-added chemicals (methanol, dimethyl ether) or fuels (methane and heavier hydrocarbons), have been reported using these two materials [12–18]. In particular, Mo₂C [19] has been reported to be a very effective catalyst for several redox transformations [12,13,20–23]. In a recent development, a two-dimensional (2D), multilayered 2D-Mo₂C material was prepared from Mo₂CT_x of the MXene family [24–26] and utilized for the hydrogenation of CO₂ into CO [27] or methane [28]. Furthermore, under heterogeneous conditions, supported molybdenum carbides or nitrides (i.e., K-Mo₂C/γ-Al₂O₃) have been found to exhibit high activity and selectivity towards CO or methane production, even at large scale (*ca.* 1 kg catalyst), with the C/Mo ratio in their structure [29–31] (Scheme 1A) playing an important role. In this context, Mo₂C was used as an efficient catalyst for the selective transfer hydrogenation process of nitroarenes into the corresponding anilines in the presence of hydrazine [32].



Scheme 1. Molybdenum carbide as catalyst for (A) selective reduction processes, (B) Photothermal/Chemodynamic Therapy (PTT/CDT) study, and (C) selective oxygenation of alkenes.

Except for the reported reductive transformations, recently, Mo₂C and W₂C were successfully used as efficient hydrogen evolution electrocatalysts [33], as well as highly sensitive biomimetic sensors of H₂O₂ [34]. Under similar oxidative conditions (in the presence of H₂O₂), Mo₂C (Mo²⁺) was transformed into Mo₂C-derived polyoxometalate clusters, i.e., Mo-POMs (Mo^{5+/6+}) [35], and then used as Photothermal/Chemodynamic Therapy (PTT/CDT) dual-agents (Scheme 1B) [36]. As reported, the resulting Mo-POMs exhibited enhanced NIR-II absorption (1060 nm) and caused massive generation of singlet oxygen (¹O₂) [36,37]. In a biomimetic scenario, glutathione (GSH) was used for the reduction of the in situ oxidized Mo-POM species, enhancing their catalytic activity. Besides these interesting applications, so far, only one other study has focused on the influence of metal carbides on oxidation processes, in particular, the oxidation of 1-octene by O₂ and *tert*-butyl hydroperoxide [38]. Considering the rare reports on Mo₂C-catalyzed oxygenation procedures, and given our interest in developing novel catalytic protocols for the oxidation of unsaturated hydrocarbons using POM-based catalysts [39–41] or Cu(I)-based (i.e., [Cu(Xantphos)(neoc)]BF₄) photocatalytic conditions [42], we report herein that Mo₂C, in the presence of H₂O₂, is a very efficient pre-catalyst that facilitates, through the in situ formation of ¹O₂, the selective C-H allylic oxygenation of alkenes and terpenoids. Numerous oxygenation processes using in situ-generated ¹O₂ by visible light photoexcitation of organic dyes have been reported in the literature [43–56]. However, to the best of our knowledge, this is the first protocol that utilizes Mo₂C, which allows the synthesis of an extended library of allylic alcohols, starting with cycloalkenes, styrenes, terpenoids and unsaturated fatty acid methyl esters under mild conditions (Scheme 1C). The conditions described herein have also been successfully applied to the laboratory-scale oxygenation of the commonly used natural compounds [57–60] β-citronellol and linalool.

2. Materials and Methods

Mo₂C was purchased from abcr (particles size 2.5–3.5 micro, >99%); H₂O₂ (30% w/v in water) was purchased from Panreac; NH₃ (25% wt in water) was purchased from VWR Chemicals; The inorganic and organic compounds were purchased from TCI, Fluka and Sigma-Aldrich. All materials and solvents were used without further purification. [Bu₄N]₄W₁₀O₃₂ was synthesized according to a method described in the literature [39]. The photo-catalyzed oxygenation of **5** using Rose Bengal and [Bu₄N]₄W₁₀O₃₂ was performed according to the synthetic procedures described in [61–63].

Preparation of Mo-POM ([Mo₆O₁₉]^{2−}) catalytic system [37]. To a solution of Mo₂C (9.8 mmol, 2 g) in distilled H₂O (15 mL) was added dropwise 2 mL of 30% w/v H₂O₂ (17.5 mmol) solution in water over a period of 30 min, and the reaction mixture was stirred at room temperature for 24 h. During H₂O₂ addition, the reaction mixture was cooled with a water bath at ca. 30 °C (it is an exothermic reaction). Next, the residual Mo₂C was removed by centrifugation, and the formed Mo-POM was obtained as a blue powder upon lyophilization (900 mg). FTIR (KBr, cm^{−1}): 3401(mbr), 1709(w), 1622(wbr), 1400(w), 959(m), 914(m), 748(mbr), 560(m). UV-Vis (CH₃CN), λ_{max}/nm: 321, 384. HR-MS (ESI) spectrum of Mo-POM [Mo₆O₁₉^{2−}] negative, calcd for Mo₆O₁₉: (z = 1) calcd m/z 879.6130, found 880.3119 and (z = 2) calcd m/z 439.8065, found 439.6546.

Preparation of [Bu₄N]_xMo-POM ([Bu₄N]₂[Mo₆O₁₉]) catalytic system. A solution of Mo-POM (360 mg) in distilled H₂O (2.5 mL) was heated to reflux. Next, a solution of tetrabutylammonium bromide (Bu₄NBr) (480 mg) in distilled H₂O (0.5 mL) was added dropwise over a period of 5 min and the precipitation of a blue powder was observed after a few minutes. After 15 min, the mixture was filtered through a vacuum Buchner apparatus and the filter cake washed with hot distilled water (2 mL), ethanol (2 mL) and diethyl ether (3 mL). The final solid material was left to dry over air in a dark place to afford [Bu₄N]_xMo-POM catalyst as a blue powder (505 mg). FTIR (KBr, cm^{−1}): 3392(mbr), 2961(m), 2873(m), 1708(w), 1622(m), 1469(m), 1380(m), 1172(w), 1152(w), 1108(w), 1063(w), 1033(w), 955(s), 877(w), 800(sbr), 655(mbr), 566(mbr), 434(w). UV-Vis (CH₃CN), λ_{max}/nm: 311, 738.

Preparation of [Et₄N]_xMo-POM ([Et₄N]₂[Mo₆O₁₉]) catalytic system. A solution of Mo-POM (200 mg) in distilled H₂O (1.5 mL) was heated up to reflux. Next, a solution of tetraethylammonium bromide (Et₄NBr) (210 mg) in distilled H₂O (0.5 mL) was added dropwise over a period of 5 min and the precipitation of a blue powder was observed after a few minutes. After 15 min, the mixture was filtered through a vacuum Buchner apparatus and the filter cake washed with hot distilled water (2 mL), ethanol (2 mL) and diethyl ether (3 mL). The final solid material was left to dry over air in a dark place to afford [Et₄N]_xMo-POM catalyst as a blue powder (251 mg). FTIR (KBr, cm^{−1}): 3152(br), 1615(m), 1459(m), 1393(w), 1183(m), 965(sbr), 913(w), 751(sbr), 650(mbr), 563(m), 435(w). UV-Vis (CH₃CN), λ_{max}/nm: 313, 753.

Oxygenation of 1-substituted cycloalkenes and dimethyl styrenes. Method A: To a solution of the corresponding alkene (0.05 mmol) in a mixture of acetonitrile/water (0.5 mL/0.1 mL) were added 25% aq. NH₃ (5 equiv., 0.25 mmol, 20 μL) and Mo-POM catalyst (ca. 10 mol%, 5 mg). Then, a solution of H₂O₂ (30% w/w) (60 equiv., 3 mmol, 300 μL) was added dropwise over a period of 15 min and the reaction mixture was stirred at room temperature for about 3 h. The reaction was monitored by thin layer chromatography (TLC), and after completion, the reaction mixture was diluted with water and extracted with ethyl acetate (2 × 2 mL). The combined organic layers were dried over MgSO₄ anhydrous, filtered and evaporated in *vacuo*. The filtrate was purified by column chromatography on silica gel by using a gradient mixture of EtOAc–Hexane to afford the corresponding allylic hydroperoxide. **Method B:** To a solution of the corresponding alkene (0.05 mmol) in a mixture of acetonitrile/water (0.5 mL/0.1 mL), 25% aq. NH₃ (5 equiv., 0.25 mmol, 20 μL) and Mo₂C (25 mol%, 2.5 mg) were added. Then, a solution of H₂O₂ (30% w/w) (60 equiv, 3 mmol, 300 μL) was added dropwise over a period of 15 min and the reaction mixture

was stirred at room temperature for about 3 h. After that, the same procedure for product isolation as described above was followed.

Oxygenation of terpenoids and methyl oleate. To a solution of the corresponding terpenoids or methyl oleate (0.05 mmol) in a mixture of acetonitrile/water (0.5 mL/0.1 mL) were added Mo₂C (25 mol%, mmol, 2.5 mg) and 25% aq. NH₃ (5 equiv., 0.25 mmol, 20 μ L). Then, a solution of H₂O₂ (30% w/w) (20 equiv., 1 mmol, 100 μ L) was added dropwise and the reaction mixture was stirred at 25 °C for about 1 h. The reaction was monitored by thin layer chromatography (TLC). After completion, the reaction mixture was diluted with water and extracted with ethyl acetate (2 \times 2 mL). The combined organic layers were dried (MgSO₄ anhydrous), filtered and evaporated in *vacuo*. The filtrate was purified by column chromatography on silica gel using a gradient mixture of EtOAc–Hexane to afford the corresponding allylic hydroperoxide.

Lab-scale oxygenation of 1-substituted cycloalkenes and dimethyl styrenes. To a solution of the corresponding alkene (1 mmol) in a mixture of acetonitrile/water (10 mL/2 mL) were added 25% aq. NH₃ (5 equiv., 5 mmol, 0.4 mL) and Mo₂C (25 mol%, 50 mg). Then, a solution of H₂O₂ (30% w/w) (60 equiv., 60 mmol, 6 mL) was added dropwise within 15 min and the reaction mixture was stirred at room temperature for about 20 h. The reaction was monitored by thin layer chromatography (TLC), and after completion, the reaction mixture was diluted with water and extracted with ethyl acetate (2 \times 5 mL). The combined organic layers were dried (MgSO₄), filtered and evaporated in *vacuo*. The filtrate was purified by column chromatography on silica gel using a gradient mixture of EtOAc–Hexane to afford the corresponding allylic hydroperoxide.

Lab-scale procedure for the oxygenation of linalool. To a solution of linalool (5 mmol, 0.9 mL) in a mixture of acetonitrile/water (50 mL/10 mL) were added Mo₂C (20 mol%, 200 mg) and 25% w/w aq. NH₃ (5 equiv., 2 mL). Then, a solution of H₂O₂ (30% w/w) (20 equiv., 11 mL) was added dropwise within 15 min under stirring at 25 °C. The reaction was monitored by thin layer chromatography (TLC), and after completion (1 h), the reaction mixture was diluted with water and extracted with ethyl acetate (2 \times 20 mL). The combined organic layers were dried over anhydrous MgSO₄, filtered and evaporated in *vacuo*. An appropriate amount of PPh₃ was added for the reduction of the OOH group into the corresponding OH. The filtrate was purified by column chromatography on silica gel using a gradient mixture of EtOAc–Hexane to afford the corresponding diols in 38% isolated yield, (320 mg).

Lab-scale procedure for the oxygenation of β -citronellol. To a solution of β -citronellol (15 mmol, 2.7 mL) in a mixture of acetonitrile/water (50 mL/10 mL) were added Mo₂C (10 mol%, 300 mg) and 25% aq. NH₃ (5 equiv., 2 mL). Then, a solution of H₂O₂ (30% w/w) (20 equiv., 33 mL) was added dropwise within 15 min and the reaction mixture was stirred at 60 °C. The reaction was monitored by thin layer chromatography (TLC), and after completion (1 h), the reaction mixture was diluted with water and extracted with ethyl acetate (2 \times 20 mL). The combined organic layers were dried over anhydrous MgSO₄, filtered and the solvent evaporated in *vacuo*. The residue was purified by column chromatography on silica gel using a gradient mixture of EtOAc–Hexane to afford the corresponding hydroperoxides in 56% isolated yield (1.620 g).

3. Results and Discussion

3.1. Evaluation and Optimization of Catalytic Conditions

Based on a recently reported study on the synthesis and utilization of a Mo₂C-derived material (Mo-POM)—which, in the presence of H₂O₂, can act as an extremely effective chemodynamic therapy (CDT) agent through the in situ formation of ¹O₂ [36]—we sought to investigate, for the first time, the potential utilization of the reported Mo-POM, generated in situ, as a catalyst for the C-H allylic oxygenation reaction of alkenes and natural compounds, such as terpenoids and fatty acid esters [64–66]. In our initial studies, Mo-POM was synthesized following the procedure described in the literature (also see also experiment part) [36]. To that end, the catalytic efficacy of Mo-POM was investigated by using 1-phenyl

cyclohexene **1** as the probe molecule. Initial control experiments were conducted for the oxygenation of **1** (0.05 mmol) by H₂O₂ (3 mmol, 60 equiv.) in the absence of Mo-POM, in CH₃CN/H₂O mixture 0.5 mL/0.1 mL (for ensuring solubility of all reagents) and using aq. NH₃ as base (0.25 mmol, 5 equiv.). However, no oxygenation products were observed by GC analysis using dodecanol as an internal standard (Table 1, entry 1). Nonetheless, in the presence of Mo-POM (5 mg), and under the same conditions, a 48% consumption of **1** was measured within 1 h reaction time, affording the allylic hydroperoxides **1a'** and **1b'** in 34% and 7% yield (ca. 5:1 ratio), respectively. The corresponding [4 + 2] cycloadduct **1c'** was formed in 9% yield (Table 1, entry 2), as determined by ¹H NMR spectroscopy [66]. By increasing the reaction time to 3 h, an almost quantitative consumption of **1** was observed with the allylic hydroperoxides **1a'** and **1b'**, forming in 61% and 12% yields, respectively (Table 1, entries 3 and 4). Meanwhile, under prolonged reactions times (up to 8 h), no significant changes were observed in the product yields (results not shown). Moreover, when the addition of H₂O₂ was made via a syringe pump apparatus (see SI) within 3 h with a constant flow rate at 100 μL/h, and allowing the process to continue for an additional 3 h, no changes on the product yields were observed by ¹H NMR spectroscopy (Table 1, entry 5). It is interesting to note that by using lower catalyst loading, no reaction completion was observed, while higher catalyst loadings did not significantly alter the reaction conversion and product yields (Table 1, entries 6–8).

Table 1. Evaluation of conditions in the Mo-catalyzed oxygenation of **1**.

Entry	Conditions ^[a]	1 % ^[b]	1a' % ^[b]	1b' % ^[b]	1c'/1d' % ^[b]
1	no catalyst/3h	100	–	–	–
2	Mo-POM (5 mg)/1 h	52	28	6	9/5
3	Mo-POM (5 mg)/2 h	25	46	9	13/7
4	Mo-POM (5 mg)/3 h	2	61	12	14/11
5 ^[c]	Mo-POM (5 mg)/3 h/syringe pump	4	59	12	16/9
6	Mo-POM (1 mg)/3 h	48	29	6	9/8
7	Mo-POM (2.5 mg)/3 h	24	44	8	14/10
8 ^[d]	Mo-POM (10 mg)/3 h	5	56	10	16/13
9	[Bu ₄ N]Mo-POM (5 mg)/3 h	2	59	12	15/12
10	[Et ₄ N]Mo-POM (5 mg)/3 h	6	57	12	13/12
11 ^[e]	Mo ₂ C (10 mol%, 1 mg)/3 h	53	26	5	9/7
12 ^[e]	Mo₂C (25 mol%, 2.5 mg)/3 h	6	58	12	14/10
13 ^[e]	Mo ₂ C (50 mol%, 5 mg)/3 h	5	55	11	16/13

^[a] (**1**) 0.05 mmol, Mo-POM (5 mg) or Mo₂C (2.5 mg, 25 mol%), aq. H₂O₂ (30% w/w) (60 equiv.), aq. NH₃ (5 equiv.), MeCN/H₂O (0.5 mL/0.1 mL), room temperature for 3 h. ^[b] Determined by the ¹H-NMR spectra of the crude reaction mixture and compared with the GC analysis after reduction of the hydroperoxides to the corresponding alcohols after the addition of Ph₃P and by using dodecanol as an internal standard. ^[c] Addition of H₂O₂ (30% w/w, 60 equiv.) via syringe pump within 3 h with a constant flow rate at 100 μL/h. ^[d] 10 equiv. of aq. NH₃ were added for maintaining pH > 10. ^[e] 0.05 mmol of **1** was used.

In an effort to determine the identity of the Mo-POM catalyst, we attempted to synthesize and isolate it in the form of the more easily handled corresponding ammonium salts, i.e., [Bu₄N]_xMo-POM and [Et₄N]_xMo-POM, through the precipitation procedure described in the experimental part. X-ray diffraction analysis data on single crystals obtained from EtOH solutions of the two ammonium salts, SEM/EDX mapping analysis, as well as high-resolution mass spectrometry (HRMS) analysis measurements (Figures S2–S5), suggested that the major species present in the isolated solids was the [Mo₆O₁₉]^{2–} polyoxometalate,

as reported earlier in the literature [67,68]. These data are in accordance with their FTIR spectra, in which the Mo=O and M-O bond stretches were observed at $\sim 960\text{ cm}^{-1}$ and $\sim 750\text{--}800\text{ cm}^{-1}$, as well as UV-Vis spectroscopy (Figures S6 and S7). Having the two ammonium salts of Mo-POM, i.e., $[\text{Bu}_4\text{N}]_x\text{Mo-POM}$ ($[\text{Bu}_4\text{N}]_2[\text{Mo}_6\text{O}_{19}]$) and $[\text{Et}_4\text{N}]_x\text{Mo-POM}$ ($[\text{Et}_4\text{N}]_2[\text{Mo}_6\text{O}_{19}]$), in hand, we further proceeded to investigate their catalytic efficacy in the above catalytic reaction. The results are summarized in Table 1 (entries 9 and 10). In both cases, similar product yields were observed by ^1H NMR of the crude reaction mixtures. These results indicated that the observed polyoxometalate was a plausible active catalytic species for the present oxygenation of **1**.

After establishing the optimum reaction conditions, we sought to study the catalyzed-oxygenation of **1** by the *in situ* prepared Mo-POM using Mo_2C directly as a pre-catalyst. Surprisingly, we found that using Mo_2C (25 mol%, 0.015 mmol, 2.5 mg) under the same conditions, the C-H allylic oxygenation of **1** (0.05 mmol) afforded products **1a'** and **1b'** in almost identical yields (Table 1, entries 11–13) with that measured after using Mo-POM (see method B in the experimental part). Based on this result, we decided to investigate, for the first time, the oxygenation of several alkenes and terpenoids into the corresponding allylic alcohols (after reduction of the initially formed hydroperoxides) under both catalytic procedures, i.e., in the presence of the isolated Mo-POM or by using Mo_2C as pre-catalyst.

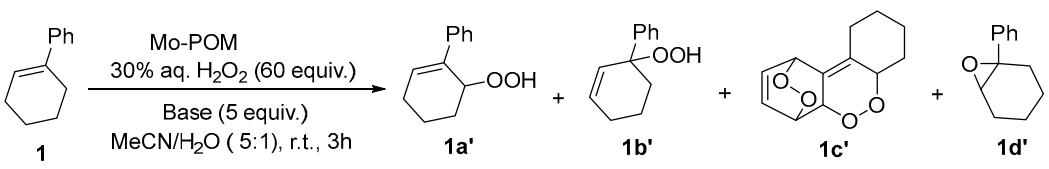
Apart from the $\text{CH}_3\text{CN}/\text{H}_2\text{O}$ 5:1 v/v mixture, different solvent mixtures were also tested, and the reaction took place efficiently in the aqueous mixtures of tetrahydrofuran (THF) and acetone (Table S1, entries 3 and 7). On the other hand, the absence or presence of a higher amount (0.5 mL) of water in acetonitrile decreased the reaction conversion (Table S1, entries 9 and 10). After that, the influence of the aqueous NH_3 amount on the reaction progress and the stability of the products was evaluated by screening different types of bases under the same reaction conditions (Table 2). Firstly, no consumption of **1** was observed in the absence of base (Table 2, entry 1); however, the aqueous solution of 25% NH_3 was found to be more suitable, affording higher product yields within 3 h (Table 2, entries 2 and 3). In addition, lower equiv. of NH_3 led to no reaction completion, while with a higher amount (10 equiv.), no reaction process was found (Table S2). Except for ammonium solutions, the presence of inorganic bases did not lead to reaction completion, while the use of Et_3N was found to promote the reaction process but with no completion (Table 2, entries 9 and 10). It is worth noting that in the presence of 5 equiv. of the organic base, an exothermic reaction was observed. According to the optimized reaction conditions (5 equiv. of aq. NH_3 and 60 equiv. of H_2O_2 and $\text{CH}_3\text{CN}/\text{H}_2\text{O}$ (5/1)), the role of H_2O_2 on the reaction progress was also tested. It was found that 60 equiv. are required to achieve higher than 95% conversion of **1**, whilst the product yields and the reaction profile were found not to be affected by higher amount of H_2O_2 or prolonged reaction time (24 h) (Table S3). Temperature-dependent experiments showed that $25\text{ }^\circ\text{C}$ is the appropriate temperature for the fast consumption of **1** within 3 h, while by increasing to $60\text{ }^\circ\text{C}$, the corresponding allylic hydroperoxides **1a'** and **1b'** were formed with similar relative yields as determined by ^1H NMR and GC after reduction with the addition of excess of PPh_3 (Table S4).

3.2. Application on the Catalytic Selective Oxygenation of Alkenes 1–19

After determining the optimal conditions, we sought to further explore the scope of the present catalytic process by the oxygenation of several 1-aryl-substituted cycloalkenes (**1–10**) and simple cycloalkenes, such as cycloheptene, cyclooctene and cyclodecene (Table 1, entry 4). Both catalytic methods, in the presence of 5 mg of Mo-POM or 2.5 mg (25 mol%) of Mo_2C (values in parentheses), were used for the selective oxygenation of **1–10** (Scheme 2) into the corresponding allylic hydroperoxides (**1a'–10a'**) as major products (see also Table S5). The corresponding secondary allylic alcohols (**1a–10a**) were isolated in moderate to good yields (50–74%) by simple chromatographic purification on SiO_2 after the *in situ* reduction of the corresponding, initially formed hydroperoxides by PPh_3 . To further investigate the generality of our catalytic protocol, Mo-POM was used as an efficient $^1\text{O}_2$ generator for the oxygenation of *cis*-1,2-dimethyl-substituted styrenes (**11–17**). In all cases,

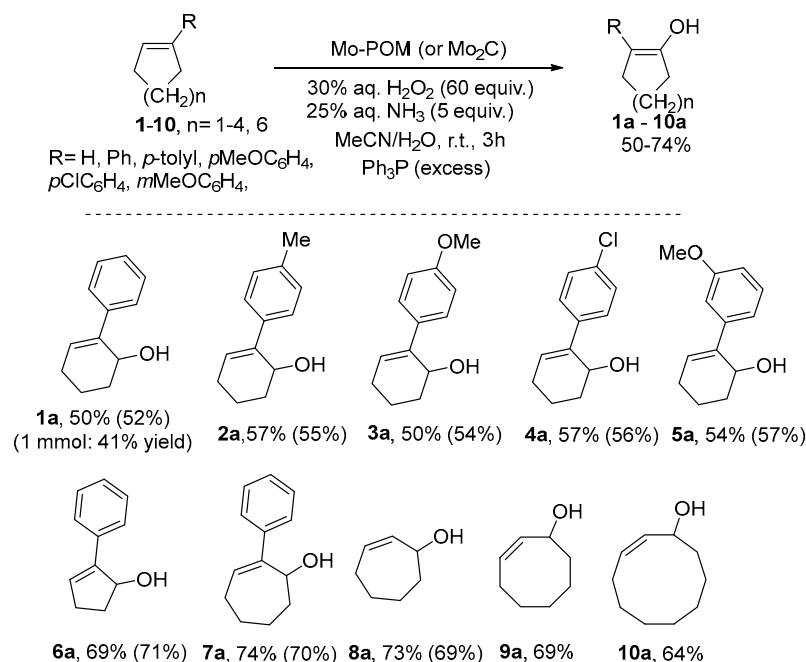
the desired allylic alcohols **11a–17a** (after addition of PPh_3) were formed in a 9/1 mole ratio with the corresponding tertiary **11b–17b** (see Table S6) and were isolated by column chromatography in good yields 63–70% (Scheme 3). Moreover, under the present catalytic conditions α,β -unsaturated alcohols **18** and **19** produced by the in situ reduction of the corresponding allylic hydroperoxides with PPh_3 were fast and quantitatively oxidized into the corresponding diols **18a** and **19a** (Scheme 3) in moderate isolated yields (67–69%).

Table 2. Base screening in the oxygenation of **1**.

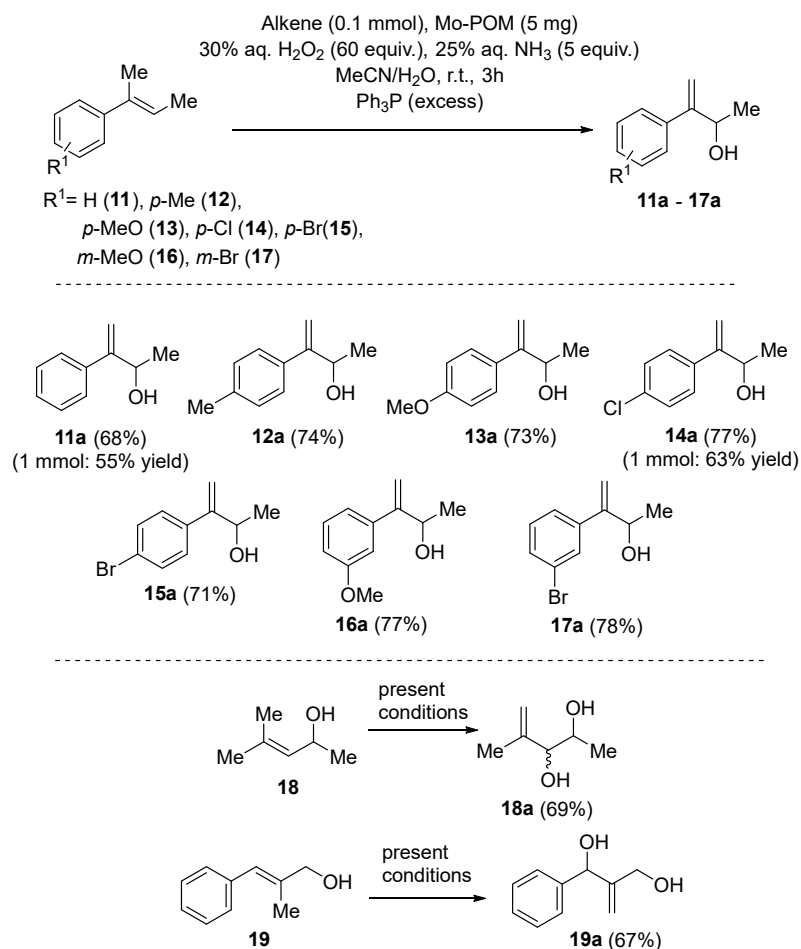


Entry	Base [a]	Yield of 1 % [b]	Yield of 1a' % [b]	Yield of 1b' % [b]	Yield of 1c'/1d' % [b]
1	–	100	–	–	–
2	10% aq. NH_3	8	55	12	15/10
3	25% aq. NH_3	2	61	12	14/11
4	10% NaOH	25	44	8	15/8
5	10% KOH	30	41	8	12/9
6	K_2CO_3	88	7	1	3/1
7	NaHCO_3	58	26	5	8/3
8	Na_2CO_3	63	21	4	7/5
9	Et_3N	21	52	10	10/7
10	Et_3N (1.5 eq)	38	39	8	9/6

[a] (**1**) 0.05 mmol, Mo-POM (5 mg), aq. H_2O_2 (30% w/w) (60 equiv.), base, (5 equiv.), MeCN/ H_2O (0.5 mL/0.1 mL), room temperature for 3 h. [b] Relative yields of products were determined by the appropriate peaks in the $^1\text{H-NMR}$ spectra of the crude reaction mixture and compared with the GC analysis after reduction of the hydroperoxides to the corresponding alcohols by the addition of PPh_3 in excess.



Scheme 2. Catalytic selective oxygenation of alkenes **1–10** in the presence of Mo-POM/ NH_3 / H_2O_2 .



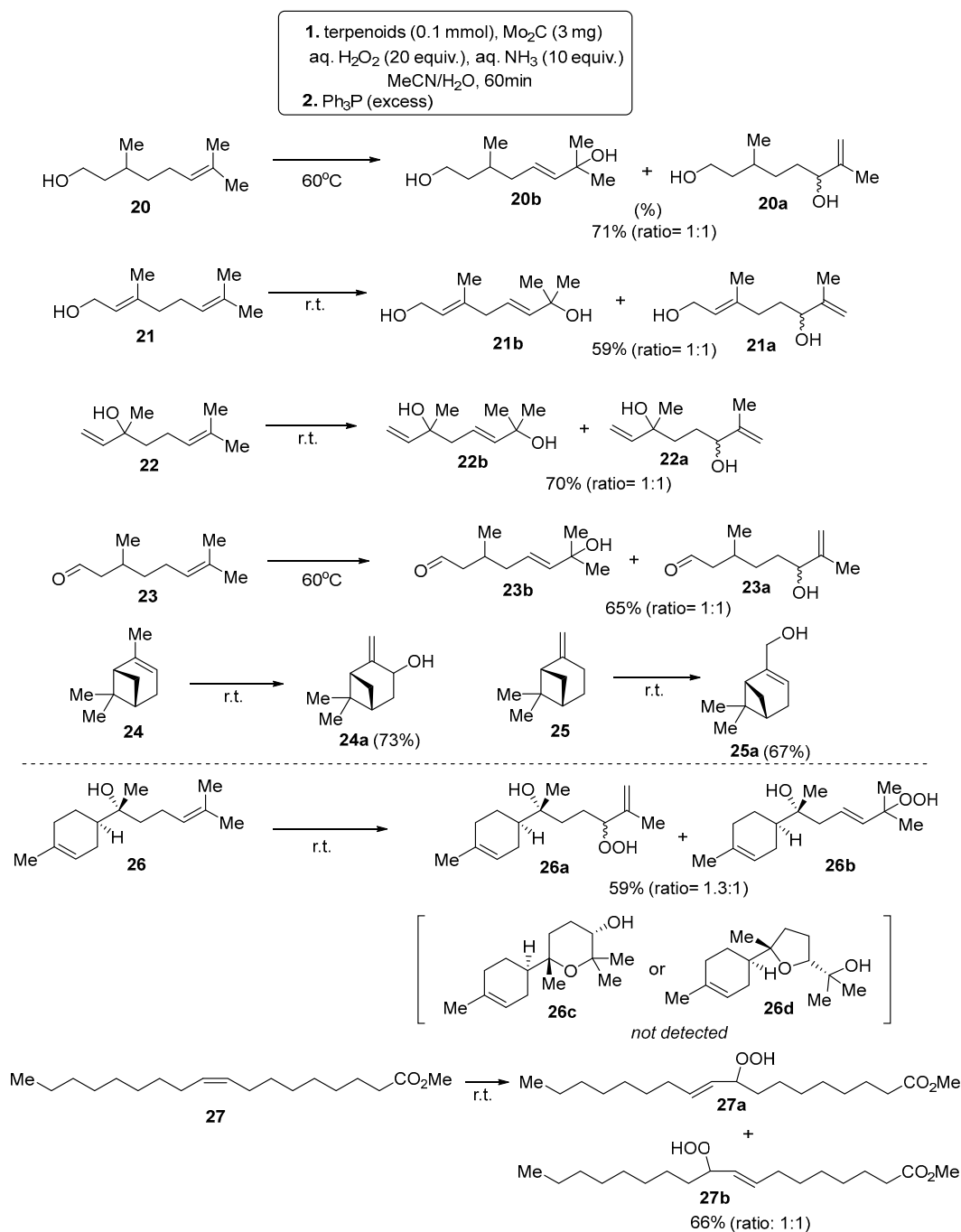
Scheme 3. Alkenes **11–19** oxygenation to the corresponding allylic alcohols **11a–19a** in the presence of Mo-POM/NH₃/H₂O₂ catalytic system.

Apart from the abovementioned cases, we also explored the possible application of the optimum reaction conditions to laboratory-scale experiments using 1 mmol of **1**, 50 mg (25 mol%) of Mo₂C and 10 mL of MeCN/H₂O (5:1), 5 mmol NH₄OH and 60 mmol of H₂O₂ (Scheme 2). The reaction process was monitored by GC. After completion (ca. 20 h), the allylic hydroperoxide **1a'** was isolated through column chromatography, reduced with the appropriate amount of PPh₃ and the corresponding allylic alcohol **1a** was finally isolated through a short pad of SiO₂ and hexane as the solvent in 41% yield, i.e., 72 mg. Further synthetic procedures using the **11** and **14** at a lab-scale were also performed, and the corresponding allylic alcohols **11a** and **14a** were isolated in 55% (82 mg) and 63% (114 mg) yields, respectively (Scheme 3).

3.3. Selective Oxygenation of Terpenoids and Lipid

We sought to extend the application of this efficient oxygenation procedure to representative examples of terpenoids (**20–25**) that are widely used in perfumes. Importantly, the reactions proceeded at the electron-rich 6,7-double bond, with high chemoselectivity toward the hydroperoxide products, while no epoxidation or alcohol moiety oxidation were observed. Interestingly, the oxygenation of terpenoids required a lower amount of H₂O₂ (20 equiv.) and shorter reaction time (60 min), leading to an equimolar mixture of the corresponding secondary and tertiary hydroperoxides in 59–71% isolated yield, or the corresponding allylic alcohols (**20a–23a** and **20b–23b**) after reduction by PPh₃ (Scheme 4). In the case of β -citronellol (**20**) and citronellal (**23**), the catalyst was shown to be highly effective at 60 °C within acetonitrile or methanol, or even ethylene glycol in a ratio of 5/1 with water (Table S7). Under the optimized conditions, α -pinene (**24**) and β -pinene (**25**)

resulted the formation of the corresponding hydroperoxides which, upon reduction with Ph_3P , afforded the corresponding allylic alcohols, i.e., **24a** and **25a**, in yields of 73% and 67%, respectively (Scheme 4).



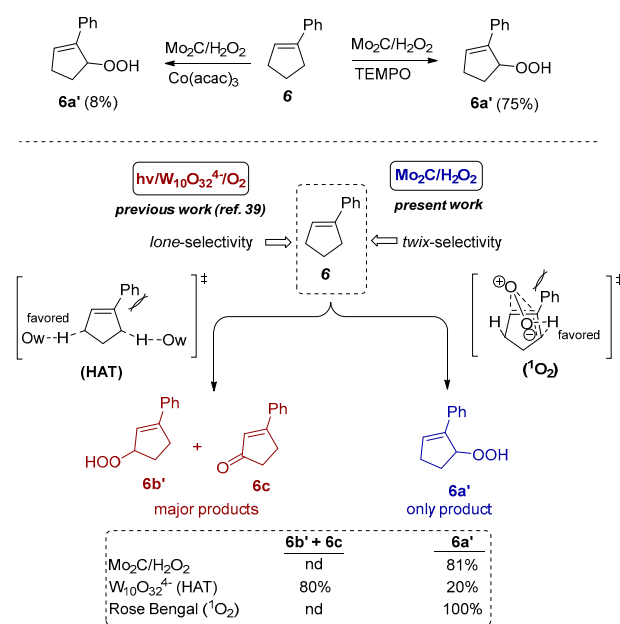
Scheme 4. Application of the present $\text{Mo}_2\text{C}/\text{NH}_3/\text{H}_2\text{O}_2$ catalytic system in the oxygenation of terpenoids and fatty acid methyl ester.

Interestingly, by using α -(-)-bisabolol (**26**) as a substrate, the oxygenation reaction afforded the desired allylic hydroperoxides in moderate isolated yield, i.e., 59% (Scheme 4); however, the corresponding α -(-)-bisabolol-oxides (**26c** and **26d**) that have been reported as oxidation products in the literature [69] were not observed among the reaction products under the present conditions. Finally, the reaction was successfully applied to the oxygenation of the methyl oleate **27**, providing access to the allylic hydroperoxides **27a** and **27b** in 1:1 ratio and in 66% isolated yield (Scheme 4). In these cases, the corresponding allylic

hydroperoxides were isolated instead of the corresponding alcohols. Laboratory-scale reactions were also tested under the present conditions using linalool (5 mmol, 0.9 mL) and β -citronellol (15 mmol, 2.7 mL) and 200 mg (20 mol%) or 300 mg (10 mol%), of the Mo_2C . In first case, the corresponding diols were isolated in 38% yield; however, in this procedure, the corresponding hydroperoxides were isolated in 56% yield (for details, see the experimental part above).

3.4. Mechanistic Study on the Selective Oxygenation of Alkene 6

To shed light on the plausible mechanism behind the present selective catalytic oxygenation process with Mo_2C , initially, experiments using **6** as starting material were performed in the presence of different quenchers. It is interesting that the presence of 1 equiv. (0.1 mmol) of the $^1\text{O}_2$ quencher $\text{Co}(\text{acac})_3$ [70] prevented the reaction progress based on the GC-analysis, while the presence of the radical inhibitor TEMPO (1 equiv., 0.1 mmol) did not significantly affect the reaction process (Scheme 5). Using the tetrabutylammonium decatungstate $[\text{Bu}_4\text{N}]_4\text{W}_{10}\text{O}_{32}$ (TBADT) as a photocatalyst [39,71,72] in the oxygenation of **6**, the corresponding allylic hydroperoxide **6a'** was observed in lower yield, i.e., 20% (Scheme 5). In contrast, the reaction shows a preference (80%) for hydrogen abstraction from the *lone* [61,62], more congested side of the double bond, yielding hydroperoxide **6b'** and the corresponding enone **6c** as major products (Scheme 5) [39]. Compound **6c** was formed by the further oxidation of the initially formed **6b'** in the presence of TBADT and O_2 [63]. This result was in line with the literature reporting non-bonding interactions (steric effects) [73] between a large group (i.e., phenyl) and an incoming decatungstate reactive intermediate (wO) in the C-H activation pathway [61]. Thus, the corresponding hydrogen atom abstraction (HAT) from the *lone*-selectivity where this steric interaction must be negligible provides a reasonable explanation for the observed side-selectivity with TBADT [74–77]. In contrast, the Mo_2C -catalyzed *twix*-selectivity (100% yield of **6a'**) reflects a complete change in mechanism with that proposed via the HAT mechanism [78–81] (Scheme 5). It is worth noting that in the photo-oxygenation with Rose Bengal, a well-known $^1\text{O}_2$ photosensitizer, i.e., **6a'** hydroperoxide, was observed as the only product, similar to the result observed with Mo_2C (81% selectivity) (Scheme 5). However, in both cases, neither **6b'** or **6c** were observed by ^1H NMR spectroscopy. These results strongly suggest that in the presence of Mo_2C , alkenes oxygenation occurred via the generation of $^1\text{O}_2$, an *in situ*-generated reactive oxygen species, as also proposed in a literature report [36].



Scheme 5. Product selectivity in the oxygenation of **6** via $\text{W}_{10}\text{O}_{32}^{4-}$ (HAT) or Mo_2C ($^1\text{O}_2$) catalysis.

4. Conclusions

In this study, we report on oxygenation reactions of organic molecules by the application of a $\text{Mo}_2\text{C}/\text{H}_2\text{O}_2/\text{NH}_3$ catalytic system, leading to the *in situ* formation of $^1\text{O}_2$. This catalytic protocol is applied to a wide range of alkenes, providing selective and efficient access to allylic alcohols via C-H activation. The amount and type of the base was found to heavily influence the reaction yield; however, NH_3 aqueous solution was found to promote the oxygenation reactions. Under the present mild conditions, terpenoids and unsaturated fatty acid methyl ester were found to be oxidized selectively, leading to the formation of the corresponding allylic alcohols after reduction. Polyoxomolybdenum anion species $\text{Mo}_6\text{O}_{19}^{2-}$ produced *in situ* during the addition of H_2O_2 into the initial solution of Mo_2C was found to be the responsible catalytic species. Finally, the performance of the catalytic system was tested at a lab-scale, affording the oxygenated products in good yields. These results support the synthetic application of this catalytic protocol. Preliminary mechanistic studies support that the $\text{Mo}_2\text{C}/\text{H}_2\text{O}_2$ -catalyzed alkene oxygenation follows the selectivity of the singlet oxygen *ene* reaction.

Supplementary Materials: The following supporting information can be downloaded at: <https://www.mdpi.com/article/10.3390/org3030014/s1>, Figures S1–S7; Tables S1–S7; NMR data and spectra.

Author Contributions: M.G.K., M.A.T. (Marina A. Tzani), D.K.G. collected the literature. M.G.K. conducted the experiments and analyzed the data together with M.A.T. (Michael A. Terzidis), D.K.G. studied the catalyst characterization and re-crystallization. P.A.A. help with the manuscript corrections and catalysts characterization. I.N.L. and M.A.T. (Michael A. Terzidis) conducted with the research idea, supervising the research project and wrote the manuscript. I.N.L. make all the manuscript corrections. All authors have read and agreed to the published version of the manuscript.

Funding: This research was funded by the Hellenic Foundation for Research and Innovation (HFRI) and the General Secretariat for Research and Innovation (GSRI), grant number [776].

Acknowledgments: The authors kindly acknowledge financial support from the Hellenic Foundation for Research and Innovation (HFRI) and the General Secretariat for Research and Innovation (GSRI) under grant agreement No. [776] “PhotoDaLu” (KA97507). The authors thank Domna Iordanidou (Aristotle University of Thessaloniki and International Hellenic University) for literature update. The authors also thanks Michael Fragkiadakis, PhD candidate at the Department of Chemistry, University of Crete, in the supervision of D. Neochoritis, for performing the ^1H and ^{13}C NMR spectra for compounds **5** and **5a**.

Conflicts of Interest: The authors declare no conflict of interest.

References

1. Ahmad, S.; Ashraf, I.; Mansoor, M.A.; Rizwan, S.; Iqba, M. An Overview of Recent Advances in the Synthesis and Applications of the Transition Metal Carbide Nanomaterials. *Nanomaterials* **2021**, *11*, 776–810. [[CrossRef](#)] [[PubMed](#)]
2. Führer, M.; van Haasterecht, T.; Bitter, J.H. Molybdenum and tungsten carbides can shine too. *Catal. Sci. Technol.* **2020**, *10*, 6089–6097. [[CrossRef](#)]
3. Sullivan, M.M.; Chen, C.-J.; Bhan, A. Catalytic deoxygenation on transition metal carbide catalysts. *Catal. Sci. Technol.* **2016**, *6*, 602–616. [[CrossRef](#)]
4. Levy, R.B.; Boudart, M. Platinum-like behavior of tungsten carbide in surface catalysis. *Science* **1973**, *181*, 547–549. [[CrossRef](#)] [[PubMed](#)]
5. Sinfelt, J.H.; Yates, D.J.C. Effect of carbiding on the hydrogenolysis activity of molybdenum. *Nat. Phys. Sci.* **1971**, *229*, 27–28. [[CrossRef](#)]
6. Li, T.; Virginie, M.; Khodakov, A.Y. Effect of potassium promotion on the structure and performance of alumina supported carburized molybdenum catalysts for Fischer-Tropsch synthesis. *Appl. Catal. Gen.* **2017**, *542*, 154–162. [[CrossRef](#)]
7. Schaidle, J.A.; Thompson, L.T. Fischer-Tropsch synthesis over early transition metal carbides and nitrides: CO activation and chain growth. *J. Catal.* **2015**, *329*, 325–334. [[CrossRef](#)]
8. Claridge, J.B.; York, A.P.E.; Brungs, A.J.; Marquez-Alvarez, C.; Sloan, J.; Tsang, S.C.; Green, M.L.H. New catalysts for the conversion of methane to synthesis gas: Molybdenum and tungsten carbide. *J. Catal.* **1998**, *180*, 85–100. [[CrossRef](#)]
9. Liu, P.; Rodriguez, J.A. Water-gas-shift reaction on molybdenum carbide surfaces: Essential role of the oxycarbide. *J. Phys. Chem. B.* **2006**, *110*, 19418–19425. [[CrossRef](#)]

10. Viñes, F.; Rodriguez, J.A.; Liu, P.; Illas, F. Catalyst size matters: Tuning the molecular mechanism of the water–gas shift reaction on titanium carbide based compounds. *J. Catal.* **2008**, *260*, 103–112. [[CrossRef](#)]
11. Akopyan, A.V.; Polikarpova, P.D.; Forofontova, O.I.; Levin, I.; Mnatsakanyan, R.A.; Davtyan, D.A.; Zurnachyan, A.; Anisimov, A.V.; Karakhanov, E.A. Hydrogenation of alkenes on Molybdenum and Tungsten carbides. *Theor. Found. Chem. Eng.* **2020**, *54*, 1045–1051. [[CrossRef](#)]
12. Porosoff, M.D.; Yang, X.; Boscoboinik, J.A.; Chen, J.G. Molybdenum carbide as alternative catalysts to precious metals for highly selective reduction of CO₂ to CO. *Angew. Chem. Int. Ed.* **2014**, *53*, 6705–6709. [[CrossRef](#)] [[PubMed](#)]
13. Posada-Pérez, S.; Vines, F.; Ramirez, P.J.; Vidal, A.B.; Rodriguez, J.A.; Illas, F. The bending machine: CO₂ activation and hydrogenation on δ -MoC(001) and β -Mo₂C(001) surfaces. *Phys. Chem. Chem. Phys.* **2014**, *16*, 14912–14921. [[CrossRef](#)] [[PubMed](#)]
14. Aresta, M. *Carbon Dioxide Recovery and Utilization*; Springer: Berlin/Heidelberg, Germany, 2013.
15. De, S.; Dokania, A.; Ramirez, A.; Gascon, J. Advances in the design of heterogeneous catalysts and thermocatalytic processes for CO₂ utilization. *ACS Catal.* **2020**, *10*, 14147–14185. [[CrossRef](#)]
16. Porosoff, M.D.; Yan, B.; Chen, J.G. Catalytic reduction of CO₂ by H₂ for synthesis of CO, methanol and hydrocarbons: Challenges and opportunities. *Energy Environ. Sci.* **2016**, *9*, 62–73. [[CrossRef](#)]
17. Wang, J.; Li, J.; Li, J.; Tang, C.; Feng, Z.; An, H.; Liu, H.; Liu, T.; Li, C. A highly selective and stable ZnO-ZrO₂ solid solution catalyst for CO₂ hydrogenation to methanol. *Sci. Adv.* **2017**, *3*, e1701290. [[CrossRef](#)] [[PubMed](#)]
18. Saeidi, S.; Amin, N.A.S.; Rahimpour, M.R. Hydrogenation of CO₂ to value added products—A review and potential future developments. *J. CO₂ Util.* **2014**, *5*, 66–81. [[CrossRef](#)]
19. Ma, Y.; Guana, G.; Hao, X.; Cao, J.; Abudula, A. Molybdenum carbide as alternative catalyst for hydrogen production. *Renew. Sustain. Energy Rev.* **2017**, *75*, 1101–1129. [[CrossRef](#)]
20. Kuo, K.; Hagg, G.A. New Molybdenum Carbide. *Nature* **1952**, *170*, 245–246. [[CrossRef](#)]
21. Zhang, X.; Zhu, X.; Lin, L.; Yao, S.; Zhang, M.; Liu, X.; Wang, X.; Li, Y.-W.; Shi, C.; Ma, D. Highly dispersed copper over β -Mo₂C as an efficient and stable catalyst for the reverse water gas shift (RWGS) reaction. *ACS Catal.* **2017**, *7*, 912–918. [[CrossRef](#)]
22. Posada-Pérez, S.; Ramirez, P.J.; Gutierrez, R.A.; Stacchiola, D.J.; Vines, F.; Liu, P.; Illas, F.; Rodriguez, J.A. The conversion of CO₂ to methanol on orthorhombic β -Mo₂C and Cu/ β -Mo₂C catalysts: Mechanism for admetal induced change in the selectivity and activity. *Catal. Sci. Technol.* **2016**, *6*, 6766–6777. [[CrossRef](#)]
23. Liu, X.; Kunkel, C.; Ramirez de la Piscina, P.; Homs, N.; Vines, F.; Illas, F. Effective and highly selective CO generation from CO₂ using a polycrystalline α -Mo₂C catalyst. *ACS Catal.* **2017**, *7*, 4323–4335. [[CrossRef](#)]
24. Naguib, M.; Gogotsi, Y. Synthesis of two-dimensional materials by selective extraction. *Acc. Chem. Res.* **2015**, *48*, 128–135. [[CrossRef](#)] [[PubMed](#)]
25. Li, Z.; Wu, Y. 2D early transition metal carbides (MXenes) for catalysis. *Small* **2019**, *15*, 1804736. [[CrossRef](#)] [[PubMed](#)]
26. Shirvani, S.; Ghashghae, M.; Smith, K.J. Two-dimensional nanomaterials in thermocatalytic reactions: Transition metal dichalcogenides, metal phosphorus trichalcogenides and MXenes. *Catal. Rev.* **2021**, 1–51. [[CrossRef](#)]
27. Zhou, H.; Chen, Z.; Kountoupi, E.; Tsoukalou, A.; Abdala, P.M.; Florian, P.; Fedorov, A.; Müller, C.R. Two-dimensional molybdenum carbide 2D-Mo₂C as a superior catalyst for CO₂ hydrogenation. *Nat. Commun.* **2021**, *12*, 5510–5519. [[CrossRef](#)]
28. Kurlov, A.; Deeva, E.B.; Abdala, P.M.; Lebedev, D.; Tsoukalou, A.; Comas-Vives, A.; Fedorov, A.; Müller, C.R. Exploiting two-dimensional morphology of molybdenum oxycarbide to enable efficient catalytic dry reforming of methane. *Nat. Commun.* **2020**, *11*, 4920. [[CrossRef](#)]
29. Juneau, M.; Vonglis, M.; Hartvigsen, J.; Frost, L.; Bayerl, D.; Dixit, M.; Mpourmpakis, G.; Morse, J.R.; Baldwin, J.W.; Willauer, H.D.; et al. Assessing the viability of K-Mo₂C for reverse water–gas shift scale-up: Molecular to laboratory to pilot scale. *Energy Environ. Sci.* **2020**, *13*, 2524–2539. [[CrossRef](#)]
30. Figueras, M.; Gutiérrez, R.A.; Viñes, F.; Ramírez, P.J.; Rodriguez, J.A.; Illas, F. Supported molybdenum carbide nanoparticles as an excellent catalyst for CO₂ hydrogenation. *ACS Catal.* **2021**, *11*, 9679–9687. [[CrossRef](#)]
31. Hamdan, M.A.; Nassereddine, A.; Checa, R.; Jahjah, M.; Pinel, C.; Piccolo, L.; Perret, N. Supported molybdenum carbide and nitride catalysts for carbon dioxide hydrogenation. *Front. Chem.* **2020**, *8*, 452–463. [[CrossRef](#)]
32. Liu, Z.; Wang, X.; Zou, X.; Lu, X. Molybdenum Carbide Catalysts for Chemoselective Transfer Hydrogenation of Nitroarenes. *ChemistrySelect* **2018**, *3*, 5165–5168. [[CrossRef](#)]
33. Chen, W.F.; Muckerman, J.T.; Fujita, E. Recent developments in transition metal carbides and nitrides as hydrogen evolution electrocatalysts. *Chem. Commun.* **2013**, *49*, 8896–8909.
34. Li, J.; Tang, C.; Liang, T.; Tang, C.; Lv, X.; Tang, K.; Li, C.M. Porous Molybdenum Carbide Nanostructured Catalyst toward Highly Sensitive Biomimetic Sensing of H₂O. *Electroanalysis* **2020**, *32*, 1243–1250. [[CrossRef](#)]
35. Nakajima, H.; Kudo, T.; Mizuno, N. Reaction of Metal, Carbide, and Nitride of Tungsten with Hydrogen Peroxide Characterized by ¹⁸³W Nuclear Magnetic Resonance and Raman Spectroscopy. *Chem. Mater.* **1999**, *11*, 691–697. [[CrossRef](#)]
36. Liu, G.; Zhu, J.; Guo, H.; Sun, A.; Chen, P.; Xi, L.; Huang, W.; Song, X.; Dong, X. Mo₂C-Derived Polyoxometalate for NIR-II Photoacoustic Imaging-Guided Chemodynamic/Photothermal Synergistic Therapy. *Angew. Chem. Int. Ed.* **2019**, *58*, 18641–18646. [[CrossRef](#)]
37. Tzani, M.A.; Gioftsidou, D.K.; Kallitsakis, M.G.; Pliatsios, N.V.; Kalogiouri, N.P.; Angaridis, P.A.; Lykakis, I.N.; Terzidis, M.A. Direct and Indirect Chemiluminescence: Reactions, Mechanisms and Challenges. *Molecules* **2021**, *26*, 7664. [[CrossRef](#)]

38. Makota, O.; Bulgakova, L. The Influence of Metal Carbides on the Oxidation Processes of 1-Octene by Molecular Oxygen and tert-Butyl Hydroperoxide. *Int. Sch. Res. Netw. ISRN Phys. Chem.* **2012**, *2012*, 135028. [[CrossRef](#)]
39. Tzirakis, M.D.; Lykakis, I.N.; Orfanopoulos, M. Decatungstate as an Efficient Photocatalyst in Organic Chemistry. *Chem. Soc. Rev.* **2009**, *38*, 2609–2621. [[CrossRef](#)]
40. Symeonidis, T.S.; Athanasoulis, A.; Ishii, R.; Uozumi, Y.; Yamada, Y.M.A.; Lykakis, I.N. Photocatalytic Aerobic Oxidation of Alkenes into Epoxides or Chlorohydrins Promoted by a Polymer-Supported Decatungstate Catalyst. *ChemPhotoChem* **2017**, *1*, 479–484. [[CrossRef](#)]
41. Tzani, M.A.; Fountoulaki, S.; Lykakis, I.N. Polyoxometalate-Driven Ease Conversion of Valuable Furfural to trans-N,N-4,5-Diaminocyclopenten-2-ones. *J. Org. Chem.* **2022**, *87*, 2601–2615. [[CrossRef](#)]
42. Kallitsakis, M.G.; Gioftsidou, D.K.; Tzani, M.A.; Angaridis, P.A.; Terzidis, M.A.; Lykakis, I.N. Selective C–H Allylic Oxygenation of Cycloalkenes and Terpenoids Photosensitized by [Cu(Xantphos)(neoc)]BF₄. *J. Org. Chem.* **2021**, *86*, 13503–13513. [[CrossRef](#)] [[PubMed](#)]
43. Orfanopoulos, M. Singlet Oxygen: Discovery, Chemistry, C₆₀-Sensitization. *Photochem. Photobiol.* **2021**, *97*, 1182–1218. [[CrossRef](#)] [[PubMed](#)]
44. Schenck, G.O. Photosensitization. *Ind. Eng. Chem.* **1963**, *55*, 40–43. [[CrossRef](#)]
45. Frimer, A.A. The Reaction of Singlet Oxygen with Olefins: The Question of Mechanism. *Chem. Rev.* **1979**, *79*, 359–387. [[CrossRef](#)]
46. Stephenson, L.M.; Grdina, M.J.; Orfanopoulos, M. Mechanism of the Ene Reaction Between Singlet Oxygen and Olefins. *Acc. Chem. Res.* **1980**, *13*, 419–425. [[CrossRef](#)]
47. Tanielian, C.; Mechin, R.; Seghrouchni, R.; Schweitzer, C. Mechanistic and Kinetic Aspects of Photosensitization in the Presence of Oxygen. *Photochem. Photobiol.* **2000**, *71*, 12–19. [[CrossRef](#)]
48. Cambié, D.; Bottecchia, C.; Straathof, N.J.W.; Hessel, V.; Noël, T. Applications of Continuous-Flow Photochemistry in Organic Synthesis, Material Science, and Water Treatment. *Chem. Rev.* **2016**, *116*, 10276–10341. [[CrossRef](#)] [[PubMed](#)]
49. Clennan, E.L. New Mechanistic and Synthetic Aspects of Singlet Oxygen Chemistry. *Tetrahedron* **2000**, *56*, 9151–9179. [[CrossRef](#)]
50. Greer, A. Christopher Foote's Discovery of Oxidation Reactions. *Acc. Chem. Res.* **2006**, *39*, 797–804. [[CrossRef](#)]
51. Alberti, M.N.; Orfanopoulos, M. Unraveling the Mechanism of the Singlet Oxygen Ene Reaction: Recent Computational and Experimental Approaches. *Chem.—A Eur. J.* **2010**, *16*, 9414–9421. [[CrossRef](#)]
52. You, Y. Chemical Tools for the Generation and Detection of Singlet Oxygen. *Org. Biomol. Chem.* **2018**, *16*, 4044–4060. [[CrossRef](#)] [[PubMed](#)]
53. Stratakis, M.; Orfanopoulos, M. Regioselectivity in the Ene Reaction of Singlet Oxygen with Alkenes. *Tetrahedron* **2000**, *56*, 1595–1615. [[CrossRef](#)]
54. Bayer, P.; Jacobi Von Wangelin, A. An Entirely Solvent-Free Photooxygenation of Olefins under Continuous Flow Conditions. *Green Chem.* **2020**, *22*, 2359–2364. [[CrossRef](#)]
55. Flors, C.; Griesbeck, A.G.; Vassilikogiannakis, G. Singlet Oxygen: Chemistry, Applications and Challenges Ahead. *ChemPhotoChem* **2018**, *2*, 510–511. [[CrossRef](#)]
56. Kopetzki, D.; Lévesque, F.; Seeberger, P.H. A Continuous-Flow Process for the Synthesis of Artemisinin. *Chem. Eur. J.* **2013**, *19*, 5450–5456. [[CrossRef](#)]
57. Margaros, I.; Montagnon, T.; Tofi, M.; Pavlakos, E.; Vassilikogiannakis, G. The Power of Singlet Oxygen Chemistry in Biomimetic Syntheses. *Tetrahedron* **2006**, *62*, 5308–5317. [[CrossRef](#)]
58. Ghogare, A.A.; Greer, A. Using Singlet Oxygen to Synthesize Natural Products and Drugs. *Chem. Rev.* **2016**, *116*, 9994–10034. [[CrossRef](#)]
59. Jefford, C.W.; Boschung, A.F.; Moriaty, R.M.; Rimbault, C.G.; Laffer, M.H. The Reaction of Singlet Oxygen with α - and β -Pinenes. *Helvetica Chimica Acta* **1973**, *56*, 2649–2659. [[CrossRef](#)]
60. Di Mascio, P.; Martinez, G.R.; Miyamoto, S.; Ronsein, G.E.; Medeiros, M.H.G.; Cadet, J. Singlet Molecular Oxygen Reactions with Nucleic Acids, Lipids, and Proteins. *Chem. Rev.* **2019**, *119*, 2043–2086. [[CrossRef](#)]
61. Lykakis, I.N.; Orfanopoulos, M. Lone Selectivity of the Decatungstate-Sensitized Photooxidation of 1-Substituted Cycloalkenes. *Syn. Lett.* **2004**, *12*, 2131–2134.
62. Lykakis, I.N.; Vougioukalakis, G.C.; Orfanopoulos, M. Homogeneous Decatungstate-Catalyzed Photooxygenation of Tetrasubstituted Alkenes: A Deuterium Kinetic Isotope Effect Study. *J. Org. Chem.* **2006**, *71*, 8740–8747. [[CrossRef](#)] [[PubMed](#)]
63. Lykakis, I.N.; Orfanopoulos, M.; Tanielian, C. Decatungstate Photocatalyzed Oxidation of Aryl Alkanols. Electron Transfer or Hydrogen Abstraction Mechanism. *Org. Lett.* **2003**, *5*, 2875–2878. [[PubMed](#)]
64. Jefford, C.W.; Rimbault, C.G. The Reaction of Singlet Oxygen with 2-Phenylcycloalkenes Possessing Small and Common Rings. *Tet. Lett.* **1976**, *28*, 2479–2482. [[CrossRef](#)]
65. Stratakis, M.; Orfanopoulos, M. Regioselective Formation of Cyclic and Allylic Hydroperoxides. *Synth. Commun.* **1993**, *23*, 425–430. [[CrossRef](#)]
66. Bayer, P.; Schachtner, J.; Májek, M.; Jacobi Von Wangelin, A. Visible Light-Mediated Photo-Oxygenation of Arylcyclohexenes. *Org. Chem. Front.* **2019**, *6*, 2877–2883. [[CrossRef](#)]
67. Du, Y.; Rheingold, A.L.; Maatta, E.A. A polyoxometalate incorporating an organoimido ligand: Preparation and structure of [Mo₅O₁₈(MoNC₆H₄CH₃)₂]²⁻. *J. Am. Chem. Soc.* **1992**, *114*, 345–346. [[CrossRef](#)]

68. Yang, X.; Waters, T.; Wang, X.-B.; O'Hair, R.A.J.; Wedd, A.G.; Li, J.; Dixon, D.A.; Wang, L.-S. Photoelectron Spectroscopy of Free Polyoxoanions $\text{Mo}_6\text{O}_{19}^{2-}$ and $\text{W}_6\text{O}_{19}^{2-}$ in the Gas Phase. *J. Phys. Chem. A* **2004**, *108*, 10089–10093. [[CrossRef](#)]
69. Barrero, A.F.; Alvarez-Manzaneda, R.E.J.; Alvarez-Manjaneda, R.R. Bisabolene derivative and other constituents from *Achillea Odorata*. *Phytochemistry* **1990**, *29*, 3213–3216. [[CrossRef](#)]
70. Vidóczy, T.; Németh, S. Quenching of Singlet Oxygen by Cobalt Complexes. In *Photochemistry and Photophysics of Coordination Compounds*; Yersin, H., Vogler, A., Eds.; Springer: Berlin/Heidelberg, Germany, 1987. [[CrossRef](#)]
71. Ravelli, D.; Protti, S.; Fagnoni, M. Decatungstate Anion for Photocatalyzed 'Window Ledge' Reactions. *Acc. Chem. Res.* **2016**, *49*, 2232–2242. [[CrossRef](#)]
72. Tanielian, C. Decatungstate photocatalysis. *Coord. Chem. Rev.* **1998**, *178–180*, 1165–1181. [[CrossRef](#)]
73. Ravelli, D.; Fagnoni, M.; Fukuyama, T.; Nishikawa, T.; Ryu, I. Site-Selective C–H Functionalization by Decatungstate Anion Photocatalysis: Synergistic Control by Polar and Steric Effects Expands the Reaction Scope. *ACS Catal.* **2018**, *8*, 701–713. [[CrossRef](#)]
74. Wan, T.; Capaldo, L.; Laudadio, G.; Nyuchev, A.V.; Rincón, J.A.; García-Losada, P.; Mateos, C.; Frederick, M.O.; Nuço, M.; Noel, T. Decatungstate-Mediated C(sp³)–H Heteroarylation via Radical-Polar Crossover in Batch and Flow. *Angew. Chem. Int. Ed.* **2021**, *60*, 17893–17897. [[CrossRef](#)] [[PubMed](#)]
75. Laudadio, G.; Deng, Y.; van der Wal, K.; Ravelli, D.; Nuño, M.; Fagnoni, M.; Guthrie, D.; Sun, Y.; Noël, T. C(sp³)–H functionalizations of light hydrocarbons using decatungstate photocatalysis in flow. *Science* **2020**, *369*, 92–96. [[CrossRef](#)] [[PubMed](#)]
76. Sarver, P.J.; Bacauanu, V.; Schultz, D.M.; DiRocco, D.A.; Lam, Y.-H.; Sherer, E.C.; MacMillan, D.W.C. The merger of decatungstate and copper catalysis to enable aliphatic C(sp³)–H trifluoromethylation. *Nature* **2020**, *12*, 459–467. [[CrossRef](#)]
77. Capaldo, L.; Quadri, L.L.; Merli, D.; Ravelli, D. Photoelectrochemical cross-dehydrogenative coupling of benzothiazoles with strong aliphatic C–H bonds. *Chem. Commun.* **2021**, *57*, 4424–4427. [[CrossRef](#)]
78. Costas, M.; Massimo Bietti, M. Uncovering the complexity of simplest atom transfer reaction. *Acc. Chem. Res.* **2018**, *51*, 2601–2602. [[CrossRef](#)]
79. Capaldo, L.; Quadri, L.L.; Ravelli, D. Photocatalytic Hydrogen Atom Transfer: The Philosopher's Stone for Late-Stage Functionalization? *Green Chem.* **2020**, *22*, 3376–3396. [[CrossRef](#)]
80. Capaldo, L.; Ravelli, D. Hydrogen Atom Transfer (HAT): A Versatile Strategy for Substrate Activation in Photocatalyzed Organic Synthesis. *Eur. J. Org. Chem.* **2017**, 2056–2071. [[CrossRef](#)]
81. Protti, A.; Fagnoni, M.; Ravelli, D. Photocatalytic C–H Activation by Hydrogen-Atom Transfer in Synthesis. *ChemCatChem* **2015**, *7*, 1516–1523. [[CrossRef](#)]